# Supplementary Materials for

## Mapping pressurized volcanic fluids from induced crustal seismic velocity drops

F. Brenguier,* M. Campillo, T. Takeda, Y. Aoki, N. M. Shapiro, X. Briand, K. Emoto, H. Miyake

*Corresponding author. E-mail: florent.brenguier@ujf-grenoble.fr

Published 4 July 2014, *Science* **345**, 80 (2014)
DOI: 10.1126/science.1254073

**This PDF file includes:**

## Materials and methods

### *Recovering continuous measurements of seismic velocity changes*

Continuous crustal seismic velocity changes can be estimated by reconstructing the daily cross-correlations of continuously recorded ambient seismic noise (*6*). Here, daily vertical-vertical cross-correlation functions were obtained from stacks of 31 cross-correlations of whitened and one-bit normalized raw seismic signals of 1–hour long, overlapped by 45 minutes (frequency range, 0.1-0.9 Hz). We also averaged the cross-correlation functions over a 5-day-long moving window, to enhance the coherence between the cross-correlation functions. The moving time interval of these windows is 1 day.

As described in Clarke et al. 2011 (*20*), for a given seismic station pair, a daily velocity change measurement can be obtained by comparing a daily cross-correlation function to a reference cross-correlation function using moving-window cross spectrum (MWCS) analysis (*21*). However, the choice of an arbitrary reference, which is usually the stack of all of the daily correlation functions for a given station pair, is ambiguous, and can lead to large outliers when a daily cross-correlation and the reference function are not similar. In this study, we generalized the process of recovering continuous measurements of seismic velocity changes by avoiding the use of an arbitrary reference function. Indeed, we apply the MWCS analysis to all daily cross-correlation pairs and invert for a continuous velocity change time series for each station pair separately. This approach allows us to deal with a large number of error-prone velocity change estimates where errors are dealt within a probabilistic way.

Let us consider $ccf_i$ as a cross-correlation function that corresponds to day i. We can thus estimate a seismic velocity (v) change between day i and day j by applying the MWCS analysis to $ccf_i$ and $ccf_j$:

$$\delta v_{ij} = \frac{v_j - v_i}{v_i} = mwcs(ccf_i, ccf_j) \qquad (1).$$

In a systematic manner, we can then estimate a velocity change between all of the pairs of daily cross-correlation functions for one given station pair. This constitutes the data vector of Equation (2):

$$d = \begin{bmatrix} \delta v_{12} \\ \delta v_{13} \\ \delta v_{14} \\ \vdots \\ \delta v_{n-1n} \end{bmatrix} \qquad (2),$$

where *d* is of length $\frac{n*(n-1)}{2}$, and n is the number of daily cross-correlation functions.

Our final goal is to reconstruct the time series of the daily velocity changes. We can define these velocity changes as $\delta v_i = \frac{v_i - v_{ref}}{v_{ref}}$, with $v_{ref}$ the constant reference velocity averaged along the travel path of the studied coda waves. The series of velocity changes constitutes our model vector *m* of Equation (3):

$$m = \begin{bmatrix} \delta v_1 \\ \delta v_2 \\ \delta v_3 \\ \vdots \\ \delta v_n \end{bmatrix} \qquad (3),$$

where *m* is of length n, the number of daily cross-correlation functions.

Let us write a relation between *m* and *d:*

$$\delta v_j - \delta v_i = \frac{v_j - v_i}{v_{ref}} = \frac{v_j - v_i}{v_i} * \frac{v_i}{v_{ref}} = \delta v_{ij} * \frac{v_i}{v_{ref}} = \delta v_{ij} * (1 + \delta v_i) \qquad (4),$$

Noting that $\delta v_i$ and $\delta v_{ij}$ are small compared to 1 (on the order of $10^{-3}$), we can write at the first order the direct linear relationship between *d* and *m* as $\delta v_{ij} = \delta v_j - \delta v_i$ or d = Gm, with G being a sparse matrix of dimension [$\frac{n*(n-1)}{2}$, n]:

$$G = \begin{bmatrix} -1 & 1 & 0 & 0 & 0..... \\ -1 & 0 & 1 & 0 & 0..... \\ -1 & 0 & 0 & 1 & 0..... \\ . & & & & \\ . & & & & \\ 0 & 0 & 0 & 0 & 0...-1 \quad 1 \end{bmatrix} \qquad (5).$$

The model vector *m* can be estimated by using a Bayesian least-squares inversion, as described by Tarantola (2002) (*22*):

$$m = \left(G^t C_d^{-1} G + \alpha . C_m^{-1}\right)^{-1} G^t C_d^{-1} d \qquad (6)$$

where $C_d$ is a covariance matrix of dimension [ $\frac{n*(n-1)}{2}, \frac{n*(n-1)}{2}$ ] that describes the Gaussian uncertainties of the data vector *d*. These values correspond to the estimated uncertainties of each $\delta v_{ij}$ estimate, using the MWCS analysis.

$C_m$ is an *a priori* covariance matrix of dimension [n,n] for model vector *m*. The parameter α is a weighting coefficient. It is determined in a way that matrix $\left(G^t C_d^{-1} G\right)$ and $\left(\alpha . C_m^{-1}\right)$ have approximately the same weight. The values of $C_m$ describe for day i how $\delta v_i$ is correlated to $\delta v_j$ at day j:

$$C_{mij} = e^{\left(-|i-j| / 2\beta\right)}, \qquad (7),$$

where β is a characteristic correlation length between the model parameters $\delta v$.

Before computing the noise cross-correlations, we first whiten the raw data in the frequency range of 0.1 Hz to 0.9 Hz, and apply one-bit normalization. Figure S1 shows an example of the noise correlations for station pair ASG-SSN, located in the Mt. Fuji area about 500 km from the Tohoku-oki earthquake epicenter. Overall it shows that the pre-processing we use allows us to retrieve stable cross-correlation functions, even during the strong aftershock activity time period following the March 2011, Tohoku-oki earthquake.

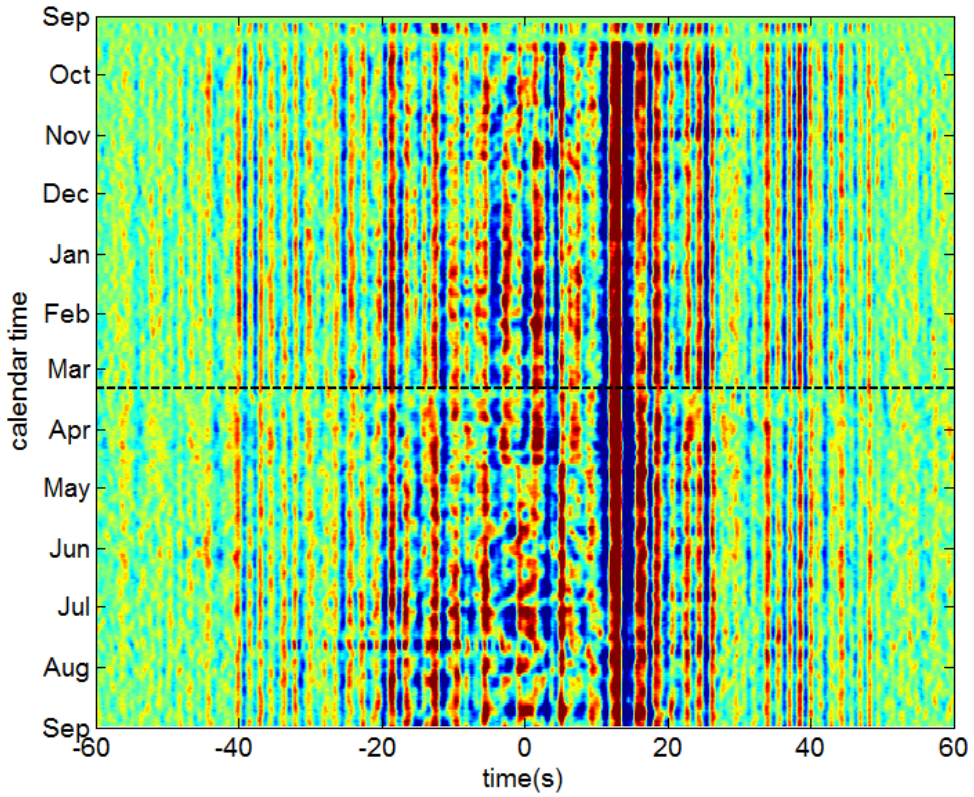


**Fig. S1.** Daily cross-correlation functions along the calendar time from Sept. 2010 (top) to Sept. 2011 for station pair ASG-SSN located in the Mt. Fuji region. We use 5-day moving window averaging to stabilize the cross-correlation functions. The black dashed line shows the time of the March 11, 2011 Tohoku earthquake.

To estimate a velocity change between cross-correlations at days i and j ($\delta v_{ij}$), we first used MWCS analysis to evaluate the time delays between the correlation functions in a series of windows centered between the direct surface-wave arrival time and a lapse time of 60 s in the coda. Each window is 10 seconds long and we overlap them by 80 %. Under the hypothesis of a uniform change in the medium, the relative velocity change is given by the slope of the function delay *versus* the lapse time (*6*).

Figure S2 shows the result of the inversion for a continuous time series of velocity changes using three different characteristic lengths of correlation between model parameters $\delta v$ ($\beta$).

Overall, we see that using a small $\beta$ value ($\beta$ = *5*), the drop of seismic velocity associated with the Tohoku-oki earthquake starts the day of the Tohoku-oki earthquake and not before, as could be misinterpreted from the velocity change time series for larger $\beta$ values. For $\beta$=5, the velocity reduction occurs on the day of the main shock because the stacked cross-correlation at a given day is an average of cross-correlations of that particular day and of the 4 previous days. Moreover, using larger $\beta$ values, we obtain highly precise velocity change curves that avoid short-term fluctuations. For information, Fig. 2A of the main manuscript is obtained using $\beta$=1000.

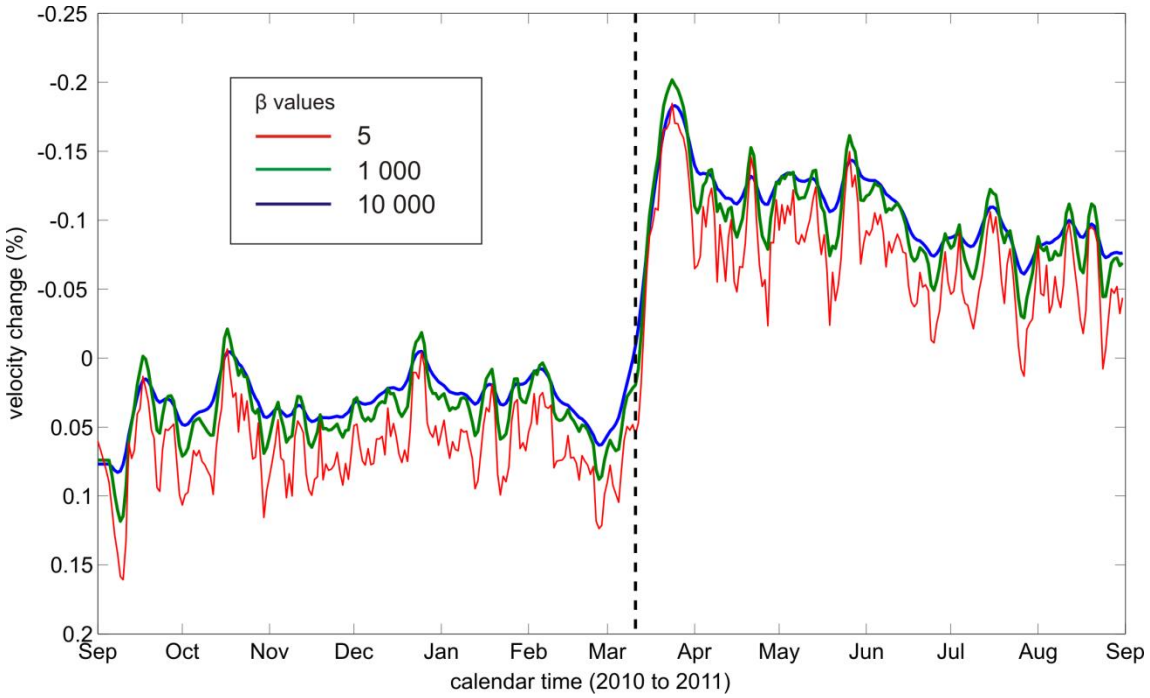


**Fig. S2.** Inverted velocity changes for station pair ASG-SSN for different values of correlations length $\beta$. The black dashed line shows the time of the March 11, 2011, Tohoku earthquake.

The errors on velocity change estimates can be assessed through the diagonal terms of the posterior covariance operator, as in Equation (8):

$$Cm_{post} = \left(G^t C_d^{-1} G + \alpha \cdot C_m^{-1}\right)^{-1} \quad (8).$$

For the results shown in Fig. S2, the errors are small compared to the background fluctuations of velocity changes (less than 0.1 %).

It is also possible to estimate how well the reconstructed velocity changes explain the data $\delta v_{ij}$ by computing the misfit function (Gm-d). For the above example, the misfit values were 0.039%, 0.04% and 0.046% for β = 5, 1000 and 10000 respectively. This shows that all three velocity change time series can explain the data $\delta v_{ij}$ well.

Finally, it is possible to compute the trace of the resolution operator, as in Equation (9):

$$R = \left(G^t C_d^{-1} G + \alpha \cdot C_m^{-1}\right)^{-1} G^t C_d^{-1} G \quad (9).$$

The trace of R gives the number of parameters resolved by the dataset in the balance with the number of parameters resolved by the *a priori* information given by $C_m$. In this example, the trace of R is 356, 162 and 56 for inversions using β = 5, 1000 and 10000, respectively. In this

case, a perfectly resolved velocity change time series would have trace(R) = 365, which is the number of days in the studied time period.

### *Mapping of velocity changes*

In this study, vertical-vertical noise correlation functions with inter-station distances <30 km were selected. According to the frequency range used (0.1-0.9 Hz), these noise correlations are very likely dominated by Rayleigh waves. Considering the sensitivity kernels of the Rayleigh waves at these frequencies (*23*), the measurements essentially characterize shear wave velocity changes averaged between the surface and about 10 km in depth.

Because we measure travel time perturbations of the coda of the reconstructed Green's functions, we can consider that the spatial sensitivity of our observations are peaked around the station positions (*24*). We can thus simply assign to each station a velocity change that is the mean of the velocity changes measured for the pairs with which a station was involved. The map of velocity changes is obtained by interpolating velocity changes at each station on a grid with 1 km of resolution. This approach allows us to directly estimate local seismic velocity changes and to perform an average of velocity changes estimates over different azimuthally distributed station pairs, thus reducing the possible bias due to non-isotropic noise-source distribution.

The Figures of the main manuscript were plotted using Generic Mapping Tool (GMT) with global multi-resolution topography (GMRT), obtained using MapTool from the Marine Geoscience Data System (*25*).

### *Static strain change computation*

Coseismic strain changes at a depth of 5 km, where the seismic waves used in the present study are the most sensitive, cannot be derived directly from observations, because all of the observations are at the surface. Here, we first invert the coseismic slip distribution from the Global Navigation Satellite System observations, and then we calculate the strain changes at a depth of 5 km from the thus-derived slip distribution.

We first processed the Global Navigation Satellite System data from 482 sites in eastern Japan, to obtain station coordinates for every second for each site. The coseismic displacements were calculated by subtracting the station coordinates from the mean between 9 min and 19 min after the main shock, to that between 1 min and 11 min before the main shock. This allowed us to eliminate the deformation due to large aftershocks, such as the one with magnitude ~8 that occurred 29 min after the main shock.

In the inversion, we assume that the observed displacements are due to the slip on the plate interface embedded in an elastic, homogeneous, and isotropic medium. The geometry of the plate interface is obtained from seismic tomography and earthquake locations, to represent a realistic and curved plate interface *(26, 27)*. The inversion is done by adaptively discretizing the plate interface so that the element sizes are smaller where the spatial resolution is better *(28)*. We do not apply any spatial smoothing, so that there is no room for the final solution to be altered by different smoothing constraints. Once the slip distribution is inverted, we can analytically estimate the strain changes at arbitrary locations and depths, because here we assume an elastic, homogeneous, and isotropic medium *(29)*.

***Mapping the seismic velocity susceptibility using observations of the peak ground velocity***

We used the KiK-net borehole accelerometers *(30, 31)* that are stored in the same tube together with the Hi-net velocity sensors *(30, 32)* to estimate the PGV. The PGV for each component was highpass filtered at 0.01 Hz, after baseline correction. We took the mean PGV over the three-components to estimate the dynamic strain/stress. Figure 2B of the main manuscript shows the seismic velocity susceptibility as the ratio between the seismic velocity changes and the dynamic stress changes. As the relationship between seismic velocity and the dynamic stress changes is likely nonlinear, and also because of the uncertainty associated with estimates of small seismic velocity and dynamic stress changes, we applied damping on the dynamic strain before computing the ratio. For the dynamic strain change computation, we changed to 10 cm/s peak ground velocity values lower than 10 cm/s.

**References and Notes**


1. S. Husen, R. B. Smith, G. P. Waite, Evidence for gas and magmatic sources beneath the Yellowstone volcanic field from seismic tomographic imaging. *J. Volcanol. Geotherm. Res.* **131**, 397–410 (2004). doi:10.1016/S0377-0273(03)00416-5

2. J. M. Lees, Seismic tomography of magmatic systems. *J. Volcanol. Geotherm. Res.* **167**, 37–56 (2007). doi:10.1016/j.jvolgeores.2007.06.008

3. D. Zhao, O. P. Mishra, R. Sanda, Influence of fluids and magma on earthquakes: Seismological evidence. *Phys. Earth Planet. Inter*. **132**, 249–267 (2002). doi:10.1016/S0031-9201(02)00082-1

4. M. E. Pritchard, J. A. Jay, F. Aron, S. T. Henderson, L. E. Lara, Subsidence at southern Andes volcanoes induced by the 2010 Maule, Chile earthquake. *Nat. Geosci.* **6**, 632–636 (2013). doi:10.1038/ngeo1855

5. Y. Takada, Y. Fukushima, Volcanic subsidence triggered by the 2011 Tohoku earthquake in Japan. *Nat. Geosci.* **6**, 637–641 (2013). doi:10.1038/ngeo1857

6. F. Brenguier, M. Campillo, C. Hadziioannou, N. M. Shapiro, R. M. Nadeau, E. Larose, Postseismic relaxation along the San Andreas fault at Parkfield from continuous seismological observations. *Science* **321**, 1478–1481 (2008). Medline doi:10.1126/science.1160943

7. See supplementary materials on *Science* Online.

8. U. Wegler, C. Sens-Schönfelder, Fault zone monitoring with passive image interferometry. *Geophys. J. Int.* **168**, 1029–1033 (2007). doi:10.1111/j.1365-246X.2006.03284.x

9. L. H. Adams, E. D. Williamson, The compressibility of minerals and rocks at high pressures. *J. Franklin Inst.* **195**, 475–529 (1923). doi:10.1016/S0016-0032(23)90314-5

10. D. A. Lockner, J. B. Walsh, J. D. Byerlee, Changes in seismic velocity and attenuation during deformation of granite. *J. Geophys. Res.* **82**, 5374–5378 (1977). doi:10.1029/JB082i033p05374

11. S. Husen, R. Taylor, R. B. Smith, H. Healser, Changes in geyser eruption behavior and remotely triggered seismicity in Yellowstone National Park produced by the 2002 M 7.9 Denali fault earthquake. Alaska. *Geology* **32**, 537–540 (2004). doi:10.1130/G20381.1

12. F. F. Pollitz, R. S. Stein, V. Sevilgen, R. Bürgmann, The 11 April 2012 east Indian Ocean earthquake triggered large aftershocks worldwide. *Nature* **490**, 250–253 (2012). Medline doi:10.1038/nature11504

13. J. L. Rubinstein, J. E. Vidale, J. Gomberg, P. Bodin, K. C. Creager, S. D. Malone, Non-volcanic tremor driven by large transient shear stresses. *Nature* **448**, 579–582 (2007). Medline doi:10.1038/nature06017

14. D. Zigone, D. Rivet, M. Radiguet, M. Campillo, C. Voisin, N. Cotte, A. Walpersdorf, N. M. Shapiro, G. Cougoulat, P. Roux, V. Kostoglodov, A. Husker, J. S. Payero, Triggering of tremors and slow slip event in Guerrero, Mexico, by the 2010 Mw 8.8 Maule, Chile, earthquake. *J. Geophys. Res.* **117**, B09304 (2012). doi:10.1029/2012JB009160

15. J. Gomberg, D. Agnew, The accuracy of seismic estimates of dynamic strains: An evaluation using strainmeter and seismometer data from Pinon Flat Observatory, California. *Bull. Seismol. Soc. Am.* **86**, 212–220 (1996).

16. B. Zinszner, P. A. Johnson, P. N. J. Rasolofosaon, Influence of change in physical state on elastic nonlinear response in rock: Significance of effective pressure and water saturation. *J. Geophys. Res.* **102**, 8105–8120 (1997). doi:10.1029/96JB03225

17. S. A. Shapiro, Elastic piezosensitivity of porous and fractured rocks. *Geophysics* **68**, 482–486 (2003). doi:10.1190/1.1567215

18. F. Hirose, K. Miyaoka, N. Hayashimoto, T. Yamazaki, M. Nakamura, Outline of the 2011 off the Pacific coast of Tohoku earthquake ($M_w$ 9.0): Seismicity: foreshocks, mainshock, aftershocks, and induced activity. *Earth Planets Space* **63**, 513–518 (2011). doi:10.5047/eps.2011.05.019

19. Y. Yukutake, R. Honda, M. Harada, T. Aketagawa, H. Ito, A. Yoshida, Remotely-triggered seismicity in the Hakone volcano following the 2011 off the Pacific coast of Tohoku Earthquake. *Earth Planets Space* **63**, 737–740 (2011). doi:10.5047/eps.2011.05.004

20. D. Clarke, L. Zaccarelli, N. M. Shapiro, F. Brenguier, Assessment of resolution and accuracy of the moving window cross spectral technique for monitoring crustal temporal variations using ambient seismic noise. *Geophys. J. Int.* **186**, 867–882 (2011). doi:10.1111/j.1365-246X.2011.05074.x

21. G. Poupinet, W. L. Ellsworth, J. Frechet, Monitoring velocity variations in the crust using earthquake doublets: An application to the Calaveras Fault, California. *J. Geophys. Res.* **89**, 5719–5731 (1984). doi:10.1029/JB089iB07p05719

22. A. Tarantola, *Inverse Problem Theory: Methods for Data Fitting and Model Parameter Estimation* (Elsevier Science, Amsterdam, 2002).

23. A. Obermann, T. Planes, E. Larose, C. Sens-Schönfelder, M. Campillo, Depth sensitivity of seismic coda waves to velocity perturbations in an elastic heterogeneous medium. *Geophys. J. Int.* **194**, 372–382 (2013). doi:10.1093/gji/ggt043

24. C. Pacheco, R. Snieder, Time-lapse travel time change of multiply scattered acoustic waves. *J. Acoust. Soc. Am.* **118**, 1300 (2005). doi:10.1121/1.2000827

25. W. B. F. Ryan, S. M. Carbotte, J. O. Coplan, S. O'Hara, A. Melkonian, R. Arko, R. A. Weissel, V. Ferrini, A. Goodwillie, F. Nitsche, J. Bonczkowski, R. Zemsky, Global multi-resolution topography synthesis. *Geochem. Geophys. Geosyst.* **10**, Q03014 (2009). doi:10.1029/2008GC002332

26. J. Nakajima, A. Hasegawa, Anomalous low-velocity zone and linear alignment of seismicity along the subducted Pacific slab beneath Kanto, Japan: Reactivation of subducted fracture zone? *Geophys. Res. Lett.* **33**, L16309 (2006). doi:10.1029/2006GL026773

27. S. Kita, T. Okada, A. Hasegawa, J. Nakajima, T. Matsuzawa, Anomalous deepening of a seismic belt in the upper-plane of the double seismic zone in the Pacific slab beneath the Hokkaido corner: Possible evidence for thermal shielding caused by subducted forearc crust materials. *Earth Planet. Sci. Lett.* **290**, 415–426 (2010). doi:10.1016/j.epsl.2009.12.038

28. Y. Aoki, "Adaptive fault discretization for the inversion of geodetic data with an application to the 2011 Tohoku-oki earthquake." Abstract S43A-2499, presented at the American Geophysical Union Fall Meeting, San Francisco, CA, 9 to 13 December 2013.

29. B. J. Meade, Algorithms for the calculation of exact displacements, strains, and stresses for triangular dislocation elements in a uniform elastic half space. *Comput. Geosci.* **33**, 1064–1075 (2007). doi:10.1016/j.cageo.2006.12.003

30. Y. Okada, K. Kasahara, K. Obara, S. Sekiguchi, H. Fujiwara, A. Yamamoto, Recent progress of seismic observation networks in Japan - Hi-net, F-net, K-NET and KiK-net. *Earth Planets Space* **56**, xv–xxviii (2004).

31. S. Aoi, T. Kunugi, H. Nakamura, H. Fujiwara, "Deployment of new strong-motion seismographs of K-NET and KiK-net." in *Earthquake Data in Engineering Seismology*, S. Akkar, P. Gülkan, T. van Eck, Eds. (Geotechnical, Geological, and Earthquake Engineering Series, Springer, Netherlands, 2011), vol. 14, pp. 167–186.

32. K. Obara, K. Kasahara, S. Hori, Y. Okada, A densely distributed high-sensitivity seismograph network in Japan: Hi-net by National Research Institute for Earth Science and Disaster Prevention. *Rev. Sci. Instrum.* **76**, 021301 (2005). doi:10.1063/1.1854197